Destructive interference between electric and toroidal dipole moments in TiO_2 cylinders and frustums with coaxial voids

IOP Conf. Series: Journal of Physics: Conf. Series **929** (2017) 012065 doi:10.1088/1742-6596/929/1/012065

Destructive interference between electric and toroidal dipole moments in TiO_2 cylinders and frustums with coaxial voids

P D Terekhov[1], K V Baryshnikova[1], A B Evlyukhin[1,2] and A S Shalin[1]

[1] ITMO University, 49 Kronversky Ave., 197101, St. Petersburg, Russia
[2] Laser Zentrum Hannover e.V., Hollerithallee, D-30419, Hannover, Germany

E-mail: terekhovpd@gmail.com

Abstract. We demonstrate numerically the possibility of multipole interference in the TiO_2 (titanium dioxide) microcylinders and microfrustums in the wavelength range 210-300 μm. Resonantly strong destructive interference between toroidal and electric dipole contributions to the scattered field is achieved by a geometry tuning. The toroidal and electric dipole mode overlapping at the resonant wavelength with almost total suppression of the total electric dipole moment is achieved.

1. Introduction

Non-radiating current configurations attract attention of physicists and engineers as possible systems for effective cloaking and camouflage [1]. In this work we consider dielectric cylinder with coaxial through hollow under plane wave irradiation. We show that in this system toroidal moment can be effectively induced. Toroidal dipole moment produces non-zero far-field radiation with a similar pattern as an electric dipole moment [2]. Interference of electric and toroidal dipole moments could be in destructive way with total suppression of far fields and reducing of the overall scattering down to the zero. We have researched similar effects for TiO_2 microcylinders in the frequency range 2-3 THz (100-150 μm) in [3]. In this work we continue our study and extend it to microfrustums with coaxial void. We obtain far-field scattering cross-section suppression in the wavelength range 210-300 μm. This frequency range allows us to perform future experiments to prove our researches.

2. Results

2.1. Main formulas

The schematics of the considered system is shown in Fig. 1 for the cylinder and in Fig. 2 for the frustum. Ordinary, usual electric dipole moment is calculated [4] as

$$\mathbf{p} = \int \mathbf{P}(\mathbf{r}')d\mathbf{r}'. \quad (1)$$

where $\mathbf{P}(\mathbf{r}')$ is a polarization vector, $\mathbf{r}'$ is the radius-vector of volume element. According to [4, 5] we calculate multipole moments including toroidal dipole moment via induced polarizations

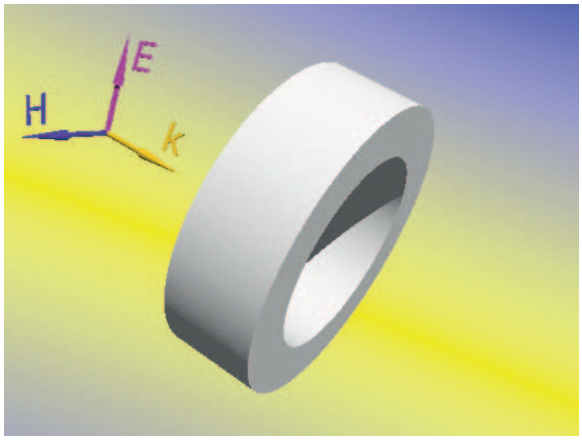

Figure 1. Cylinder, irradiated by plane wave, which propagates along the cylinder axis. **k** is the wave vector, **E** is the electric field, **H** is the maghetic field.

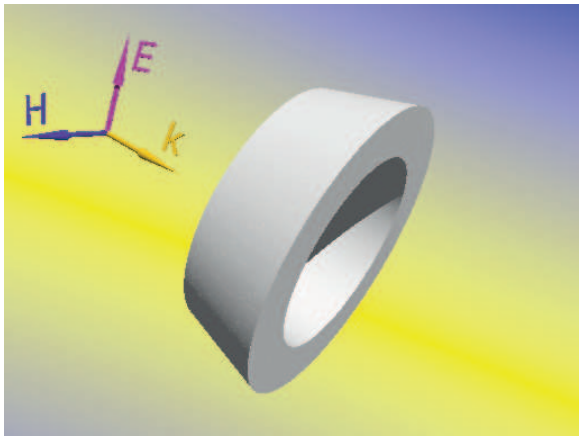

Figure 2. Frustum, irradiated by plane wave, which propagates along the cylinder axis. **k** is the wave vector, **E** is the electric field, **H** is the maghetic field.

inside scatterer (COMSOL Multiphysics). For example, toroidal dipole moment is determined as [4, 5]

$$\mathbf{T} = \frac{i\omega}{10}\int\{2\mathbf{r}'^2\mathbf{P}(\mathbf{r}') - (\mathbf{r}'\cdot\mathbf{P}(\mathbf{r}'))\mathbf{r}'\}d\mathbf{r}'. \tag{2}$$

The toroidal dipole moment is the third order multipole moment, and one can expect that its contributions rises as the particle size increases with respect to considered wavelength. In our case the particles are large enough in order to support the resonant exitation of the third order multipoles. We calculate the contribution of electric dipole (ED) and toroidal dipole (TD) moments to the scattered field in the far-field as [4, 5]

$$\mathbf{E}_{sca}(\mathbf{r}) \sim \frac{k_0^2}{4\pi\varepsilon_0}\{\mathbf{n}\times\mathbf{P}\times\mathbf{n} + \frac{ik_0\varepsilon_d}{c}\mathbf{n}\times\mathbf{T}\times\mathbf{n}\}, \tag{3}$$

where $\mathbf{r}$ is the radius-vector of an observation point; k_0 is the free-space wave number; ε_d is the relative dielectric permittivity of the surrounding medium (in our case $\varepsilon_d = 1$); ε_0 is the vacuum permittivity; c is the light speed in the vacuum; $\mathbf{n}$ is the unit vector directed along $\mathbf{r}$. Considering several multipole moments up to electric octupole the following expression for the scattering cross-section σ_{sca} was obtained (see [4] for details):

$$\begin{aligned}\sigma_{\text{sca}} \simeq\ & \frac{k_0^4}{6\pi\varepsilon_0^2|\mathbf{E}_{inc}|^2}|\mathbf{p} + \frac{ik_0\varepsilon_d}{c}\mathbf{T}|^2 + \frac{k_0^4\varepsilon_d}{6\pi\varepsilon_0|\mathbf{E}_{inc}|^2}|\mathbf{m}|^2 \\ & + \frac{k_0^6\varepsilon_d}{720\pi\varepsilon_0^2|\mathbf{E}_{inc}|^2}\sum|Q'_{\alpha\beta}|^2 + \frac{k_0^6\varepsilon_d^2}{80\pi\varepsilon_0|\mathbf{E}_{inc}|^2}\sum|M'_{\alpha\beta}|^2 \\ & + \frac{k_0^8\varepsilon_d^2}{1890\pi\varepsilon_0^2|\mathbf{E}_{inc}|^2}\sum|O'_{\alpha\beta\gamma}|^2\,.\end{aligned} \tag{4}$$

where $\mathbf{m}$ is the magnetic dipole moment (MD) of particle; $|\mathbf{p} + \frac{ik_0\varepsilon_d}{c}\mathbf{T}|$ corresponds to the interference of electric dipole and toroidal dipole moments, which can be treated as total electric dipole moment (TED); Q', M' and O' are the electric quadrupole moment tensor (EQ), the magnetic quadrupole moment tensor (MQ) and the tensor of electric octupole moment (OCT)

respectively, where $'$ means that matrices of these tensors have been symmetrized and they are traceless. Similar multipole approach up to the second order multipoles has been considered in classical textbooks [6, 7]. The third order multipoles has been taken into account in [5]. This procedure allows to obtain cross-contributions of different tensor moments to scattering equal to zero. Total scattering cross-section was obtained through the integration of Pointing vector over a closed surface in the far zone and the normalization on the incident field intensity [8]. Same multipole decomposition tehnique has been recently used to show so-called super-dipole regime in optical frequency range in [9].

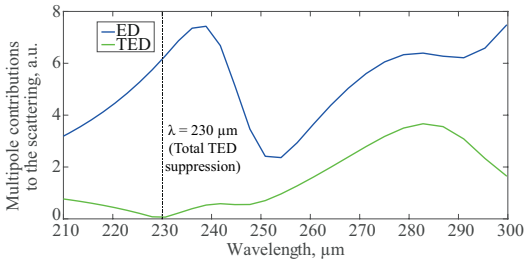

Figure 3. Absolute magnitude of electric dipole moment (blue line) and absolute magnitude of total electric dipole moment (green line) of TiO_2 cylinder, $D = 184.04\ \mu m, H = 27.64\ \mu m$, $D_{core} = 152.5\ \mu m$. The vertical black line corresponds to the wavelength of the almost total TED suppression.

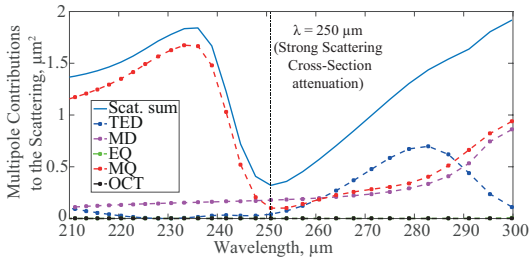

Figure 4. Scattering cross section multipole decomposition spectra for TiO_2 cylinder. $D = 184.04\ \mu m, H = 27.64\ \mu m$, $D_{core} = 152.5\ \mu m$. The dashed blue line corresponds to the TED contribution to the scattering cross-section, the dashed purple line - to the MD contribution, the dashed green line - to the EQ contribution, the dashed red line - the the MQ contribution, the dashed black line - to the OCT contribution and the solid blue line - to the total scattering cross-section.

2.2. Scattering on TiO_2 microdisks with coaxial void

In [3] we have obtained suppression of total electric dipole contribution to the far-field scattering cross section in the frequency range 2-3 THz (100-150 μm). In this work we scale this effect to the wavelength range 210-300 μm. We consider optimized microcilynder parameters and obtain two cases with same coaxial void diameter $D_{core} = 152.5\ \mu m$, same height $H = 27.64\ \mu m$ and different particle diameter $D = 184.04\ \mu m$ for the small cylinder and $D = 215.96\ \mu m$ for the big one. In Fig. 3 and 5 we present ordinary electric dipole moment and total electric dipole moment spectra for small and big cylinders respectively. In both cases we obtain the almost total suppression of total electric dipole moment due to destructive interference of electric and toroidal dipole moments at the wavelengths $\lambda = 230\ \mu m$ for the small cylinder and $\lambda = 264\ \mu m$ for the big one. Wavelengths, corresponding to the almost total suppression, are marked in Fig. 3 and 5 as vertical black lines. In Fig. 4 and 6 we present multipole decomposition of scattering cross section for small and big cylinder respectively. One can observe large magnetic quadrupole contribution. In Fig. 4 one can note significant scattering suppression due to destructive interference of electric and toroidal dipole contributions to the scattering cross-section at the wavelength $\lambda = 250\ \mu m$.

This wavelength is marked in Fig. 4 as vertical black line. Note that at the wavelengths, where TED is equal to zero, the scattering is basically determined by MQ contribution.

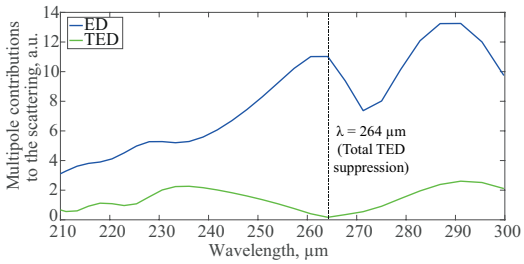

Figure 5. Absolute magnitude of electric dipole moment (blue line) and absolute magnitude of total electric dipole moment (green line) of TiO_2 cylinder, $D = 215.96\ \mu m, H = 27.64\ \mu m$, $D_{core} = 152.5\ \mu m$. The vertical black line corresponds to the wavelength of the total TED suppression.

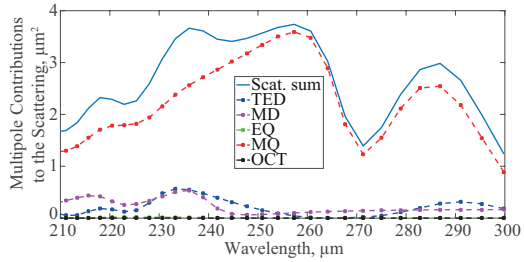

Figure 6. Scattering cross section multipole decomposition spectra for TiO_2 cylinder. $D = 215.96\ \mu m, H = 27.64\ \mu m$, $D_{core} = 152.5\ \mu m$. The dashed blue line corresponds to the TED contribution to the scattering cross-section, the dashed purple line - to the MD contribution, the dashed green line - to the EQ contribution, the dashed red line - the the MQ contribution, the dashed black line - to the OCT contribution and the solid blue line - to the total scattering cross-section.

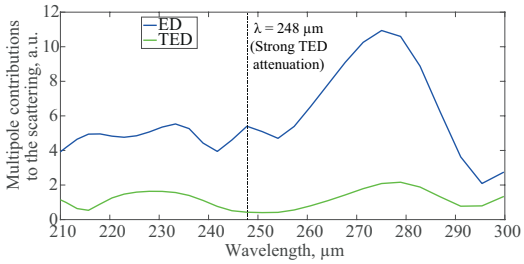

Figure 7. Absolute magnitude of electric dipole moment (blue line) and absolute magnitude of total electric dipole moment (green line) of TiO_2 frustum, $D_{top} = 215.96\ \mu m, D_{bottom} = 184.04\ \mu m$, $H = 27.64\ \mu m, D_{core} = 152.5\ \mu m$. The vertical black line corresponds to the wavelength of the strong TED attenuation.

2.3. Scattering on TiO_2 microfrustum with coaxial void

Frustum microparticles are convenient to fabricate with available equipment as well as cylindrical ones. In this work we consider frustums with coaxial void radius and height, corresponding to the previous subsection. Top frustum radius corresponds to the smaller cylinder, and the bottom radius corresponds to the bigger one. In Fig. 7 we present ordinary electric dipole moment and total electric dipole moment spectra for the TiO_2 microfrustum with $D_{top} = 215.96\ \mu m, D_{bottom} = 184.04\ \mu m, H = 27.64\ \mu m, D_{core} = 152.5\ \mu m$. It is possible to observe the minimum total electric dipole contribution to the scattering cross-section at the wavelength $\lambda = 248\ \mu m$ (marked as the vertical black line in Fig. 7. This wavelength corresponds to average value between wavelengths, corresponding to similar minimum contributions for cylinders ($\lambda = 230\ \mu m$ for the small cylinder and $\lambda = 264\ \mu m$ for the big one). However,

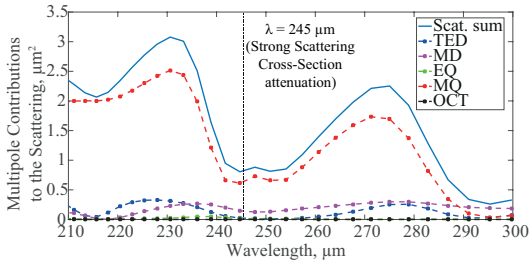

Figure 8. Scattering cross section multipole decomposition spectra for TiO_2 frustum. $D_{top} = 215.96\ \mu m, D_{bottom} = 184.04\ \mu m$, $H = 27.64\ \mu m, D_{core} = 152.5\ \mu m$. The dashed blue line corresponds to the TED contribution to the scattering cross-section, the dashed purple line - to the MD contribution, the dashed green line - to the EQ contribution, the dashed red line - the the MQ contribution, the dashed black line - to the OCT contribution and the solid blue line - to the total scattering cross-section. The vertical black line corresponds to the wavelength of strong scattering cross-section attenuation.

for the frustum microparticle one can observe not total suppression of total electric dipole moment, but its strong attenuation. Multipole decomposition of scattering cross section for considered microfrustum is presented in Fig. 8. We obtain scattering cross-section minimum at the wavelength region, corresponding to the region of total electric dipole attenuation (the vertical black line in Fig. 8). The scattering is basically determined by MQ contribution.

3. Conclusions

In conclusion, TiO_2 microcylinders and microfrustums possess multipole resonant response in the wavelength range 210-300 μm. Toroidal moment has the same contribution to the far-field scattering as electric dipole and interferes with it in destructive manner. Magnitude and resonance frequency of toroidal and electric dipole moments of the cylinder or frustum with coaxial void depends on its aspect ratio and void radius. Destructive interference of electric and toroidal dipole modes can totally destroy total electric dipole contribution to scattering. Total electric dipole moment suppression provided by microfrustum with coaxial void located on the wavelength spectrum at the region, corresponding to the average value of total electric dipole suppression effects, provided with microcylinders with coaxial voids with diameters, corresponding to top and bottom frustum diameters. Strong scattering cross-section attenuation for TiO_2 microfrustum has been obtained. Considered effect of electric dipole radiation suppression can be used in some important applications such as invisibility, optical detection and others.

Acknowledgements

This work was supported, in part, by the Russian Fund for Basic Research within the project 16-52-00112. The analytical calculation of multipolar terms has been supported by the Russian Science Foundation Grant No. 16-12-10287. A.S.S. acknowledges the support of the President of Russian Federation in the frame of Scholarship SP-4248.2016.1 and the support of Ministry of Education and Science of the Russian Federation (GOSZADANIE 2014/190). K.V.B. researching was partially supported by FASIE.

References

[1] Edwards B, Alù A, Silveirinha M G and Engheta N 2009 *Physical Review Letters* **103** 153901
[2] Miroshnichenko A E, Evlyukhin A B, Yu Y F, Bakker R M, Chipouline A, Kuznetsov A I, Lukyanchuk B, Chichkov B N and Kivshar Y S 2015 *Nature communications* **6**

[3] Terekhov P D, Baryshnikova K V, Shalin A S, Evlyukhin A B and Khromova I A 2016 Nonradiating anapole modes of dielectric particles in terahertz range *Days on Diffraction (DD), 2016* (IEEE) pp 406–409
[4] Evlyukhin A B, Fischer T, Reinhardt C and Chichkov B N 2016 *Physical Review B* **94** 205434
[5] Chen J, Ng J, Lin Z and Chan C 2011 *Nature photonics* **5** 531–534
[6] Jackson J D 1975 *Electrodynamics* (Wiley Online Library)
[7] Landau L D and Lifshitz E M 1971 *The classical theory of fields* (Pergamon)
[8] Evlyukhin A B, Reinhardt C, Evlyukhin E and Chichkov B N 2013 *JOSA B* **30** 2589–2598
[9] Terekhov P D, Baryshnikova K V, Shalin A S, Karabchevsky A and Evlyukhin A B 2017 *Optics Letters* **42** 835–838